Horticulture Advances

RESEARCH ARTICLE

Open Access

Plastid-encoded RNA polymerase variation in *Pelargonium* sect *Ciconium*

FC Breman[1], JW Korver[1], RC Snijder[2], C Villard[1], ME Schranz[1] and FT Bakker[1*]

Abstract

Cyto-Nuclear Incompatibility (CNI), in which there is a mismatch in the interaction between organelles and nucleus, impacts plant species evolution as it has a direct effect on the fitness of plants. It can reduce fertility and/or result in bleached plants devoid of functional chloroplasts. Understanding the processes leading to CNI could help to improve breeding efforts, especially in cases where species with desirable traits need to be crossed into existing cultivars. To better understand the occurrence of CNI and its effects on plant phenotype, we combined near comprehensive crossing series across a clade of species from *Pelargonium* section *Ciconium* with comparative genomics and protein modelling for plastid-encoded RNA polymerase (PEP), as the *rpo* genes encoding PEP subunits were found to be unusually highly divergent, especially in two length-variable regions. Of all plastome-encoded genes, we found these genes to contain more variation than observed across angiosperms and that this underlies structural variation inferred for PEP in *P.* sect. *Ciconium*. This variation, resulting in differing physico-chemical properties of the rpo-encoded peptides, provides a possible explanation for the observed CNI, but we cannot directly correlate plastid related CNI phenotypes to rpo genotypes. This suggests that more than one interaction between the nuclear genome and the plastome genes are needed to fully explain the observed patterns.

Keywords *Pelargonium*, Evolution, Plastid encoded polymerase, CNI, *Ciconium*

Introduction

Cyto-Nuclear Incompatibility (CNI), is the (partial) failure or breakdown in communication between nuclear and organellar genomes. It occurs when populations, derived from a single ancestor, and having become separated in space and time, undergo secondary contact. Such populations may have acquired mutations independently from each other, creating possible reproductive barriers. This is referred to as the Bateson-Dobzhansky-Muller (BDM) model of speciation (Bateson 1909; Dobzhansky 1936; Müller 1942) and is thought to underly the occurrence of CNI.

CNI can be caused by nuclear mismatch with mitochondria (mCNI) as well as with chloroplasts (pCNI). Whereas mCNI manifests itself as dwarf growth or (partial) male sterility (Schnable and Wise 1998), pCNI on the other hand, occurs as bleaching of the leaves (chlorosis), a regularly-occurring phenomenon in F_1 hybrids of interspecific crosses in, for instance, *Pelargonium* (Geraniaceae) (Baur 1909; Horn 1994; Breman et al. 2020). Angiosperm-wide, CNI has so far been reported from at least 14 genera (Greiner et al. 2011). Sharbrough et al. 2022 investigated CNI in allopolyploids and how interactions between nuclear and cytoplasmic genes are coordinated, across angiosperms. In cases of biparental inheritance of organelles (mainly plastids), the presence of a plastid incompatible with one of the parental donor genomes will induce signaling mismatches between nuclear genomic genes controlling plastid expression

*Correspondence:
FT Bakker
freek.bakker@wur.nl
[1] Biosystematics Group, Wageningen University and Research, Radix Building 107, Droevendaalsesteeg 1, 6708 PB Wageningen, the Netherlands
[2] Syngenta Seeds BV Cornelis, Kuinweg 28, 1619 PE Andijk, the Netherlands

(Postel and Touzet 2020; Canonge et al. 2021; Qin et al. 2021; Forsythe et al. 2021) and the plastome. The regulation and expression of organelles is coordinated by the nuclear genome upon light-activation of tissue (Zoschke and Bock 2018) which triggers five different pathways that co-interact with the nucleus and chloroplast in ways that are not fully understood (Zoscke and Bock 2018). For chloroplasts, the so-called anterograde (from nucleus to organelle) signals consist of nuclear encoded proteins (Tadini et al. 2020) that initially target the *rpoB* subunit of the plastid-encoded RNA polymerase (PEP) complex, which then initiates expression of plastome-encoded genes (Börner et al. 2015). The PEP complex consists of four subunits called α, β, β' and β", respectively encoded by the *rpoA*, *rpoB*, *rpoC1*, and *rpoC2* genes (Börner et al. 2015). In *Pelargonium* sect. *Ciconium* (and Geraniaceae in general), *rpo* gene sequences were found to be highly variable in length (Guisinger et al. 2008; Breman 2021) and showed signs of strong positive selection. Generally, PEP is involved in the initiation of plastome transcription and (almost) solely responsible for the expression of rRNA and photosystem I and II genes *psba* and *psbb* (Demarsy et al. 2006), as well as of tRNA (Williams-Carrier et al. 2014). All other plastid genes are, at least partially, expressed *via* the nuclear-encoded (RNA) polymerase (NEP) (Demarsy et al. 2006; Palomar et al. 2022). In contrast to the plastids, plant mitochondria do not encode their own polymerase and mitochondrial genes are expressed *via* the same NEP as used for a subset of genes in the plastids, as well as by a dedicated nuclear-encoded, mitochondrially targeted NEP (Zoschke and Bock 2018).

The commonly known 'garden geranium' (*P.* × *hortorum*) is the product of interspecific hybridization between two species from *P.* sect. *Ciconium* (Sweet) Harvey (1860: 298), *P. inquinans* and *P. zonale* (James et al. 2004) and represents a suitable model for studying CNI as it exhibits both CNI and bi-parental inheritance. Its origins date back to the 19th century, when intense hybridization efforts were undertaken since the early 1800s (*e.g.* Sweet 1820-1830), especially in Victorian England. Early breeders noticed the frequent occurrence of chlorosis in offspring of species from *P.* section *Ciconium* (hereafter referred to as '*Ciconium*'), and later it was established that aberrant chloroplast inheritance was causal (Baur 1909). Establishing interspecific hybrids between several species of *Pelargonium* is relatively easy (Horn 1994; Breman et al. 2020) making *Pelargonium* an attractive model genus for studying CNI.

Biparental inheritance of plastids appears to be not as uncommon across angiosperms as usually considered (Greiner et al. 2015). However, it appears to be particularly common in *Pelargonium,* especially in the *Ciconium* clade (Baur 1909; Metzlaff et al. 1981; Guo and Hu 1995; Weihe et al. 2009; Apitz et al. 2013). All 17 species in this clade display the ability to transmit (and accept) plastids from either parent (Breman et al. 2020). Given the ubiquity of cytoplasmic biparental inheritance in *Ciconium,* it could be more widespread throughout the genus but this has not been studied yet. The level of chlorosis in interspecific offspring in this clade was found to be dependent on the specific plastome/nuclear genome combination (Tilney-Basset 1984; Tilney-Basset et al. 1992; Breman et al. 2020).

The plastomes of *Pelargonium* species are re-arranged structurally (Röschenbleck et al. 2017) when compared to the generally conserved angiosperm plastome structure (Wicke et al. 2011). This is probably due to the frequent occurrence of small and middle-sized repeats which can act as sites for non-homologous rearrangement (Ruhlman and Jansen 2018; for a review of Geraniaceae plastome properties). In addition, *Pelargonium* plastomes are among the largest known for angiosperms (*i.e.* ~275kb for *P.* × *hortorum*, Chumley et al. 2006; Weng et al. 2012, 2017). Combined with the unusual length variation in *rpo* gene sequences outlined above, these unique features make *Ciconium* plastomes an interesting test-case for studying the genetic and molecular basis for the observed pCNI in hybrid offspring. We therefore study the inheritance of chloroplasts in interspecific *Pelargonium* crosses for the entire clade and relate chlorotic phenotypes to the unusually high PEP structural variation encountered in section *Ciconium,* also at the protein-structure level. Having the complete complement of species for a clade allows us to compare all extant structural variants and evaluate the differences in detail.

Given their roles in expression regulation by the nucleus and involvement in plastid gene transcription (Demarsy et al. 2006), we consider the *rpo* genes as relevant in explaining chlorosis. We therefore explore the possible effects of the *rpoB, rpoC1 and rpoC2* length and sequence variation in *Ciconium* species on their occurrence of CNI. We do that by describing and matching peptide physico-chemical properties and modelled peptide structures in the *Ciconium* species compared. We then explore whether correlation exists between peptide structure and chlorosis phenotypes and speculate what the structural effects could be of the observed sequence variation.

Materials and methods

Plant material, DNA extraction and sequencing

Plant material was obtained from other research (Breman et al. 2021) or collected from herbaria and living collections (Table 1). Plant DNA was extracted using an adjusted CTAB protocol (Bakker et al. 1998) followed

Table 1 Plant materials used in this study, along with herbarium voucher information

Species	Herbarium voucher accession	Institute[a]	Acronym used in text
P. acetosum	1243	STEU	ACET
P. acraeum	1975	STEU	ACRA
P. alchemilloides	1885	STEU	ALCH2x
P. alchemilloides	1882	STEU	ALCH4x
P. articulatum	1972055	WAG	ARTI
P. barklyi	1972061	WAG	BARK
P. frutetorum	0754	STEU	FRUT
P. inquinans	0682	STEU	INQU
P. multibracteatum	2902	STEU	MULT
P. peltatum	1890	STEU	PELT
P. quinquelobatum	1972049	WAG	QUIN
P. ranuncolophyllum	A3651	MSUN[b]	RANU
P. tongaense	3074	STEU	TONG
P. zonale	1896	STEU	ZONA
P. elongatum	0854	STEU	ELON
P. aridum	1847	STEU	ARID
P. insularis	19990489	RBGE	INSU
P. yemenense sp. nov	1972037	WAG	YEME
P. omanense sp. nov	2184	RBGE	OMAN
P. somalense	V-067490	V	SOMA

[a] *STEU* Stellenbosch University, *RSA; AL* Albers/MSUN=Münster

[b] Bakker et al. 2004. WAG= National Herbarium of the Netherlands. V=Uppsala herbarium

by RNAse treatment. The obtained DNA extracts were sent to Novogene Inc. (Cambridge and Hong Kong) for Illumina HiSeq sequencing. Read libraries were generated from 1.0 µg genomic DNA using the NEBNext DNA Library Prep Kit following the manufacturer's protocols, with genomic DNA randomly fragmented by shearing to ~350 bp. Fragments were subsequently subjected to end polishing, A-tailing, and ligation to the NEBNext adapter for Illumina HiSeq sequencing (Illumina, Inc. San Diego, USA) (Breman et al. 2021) with an average coverage of 0.5–1 X. Throughout the text we use four-letter-acronyms for each accession used, see Table 1 for the corresponding species names.

Establishment of four F_1 crossing series

Methods for generating and establishing F_1 hybrids in this study were described in past research (Breman et al. 2020) for the domesticated *P.* × *hortorum* crossing series. We generated three additional crossing series, including three wild species representing phylogenetic diversity across the *Ciconium* clade (van de Kerke et al. 2019) and with which we crossed all available section members (Table 1). The three wild species used were: *P. barklyi* ('BARK'), *P. multibracteatum* ('MULT') and *P. acetosum*, ('ACET'), who were placed in different clades in our repeatome-based phylogenetic tree (Breman et al. 2021). A visual overview of the total of four crossing series (including *P.* × *hortorum*) is given in Fig. 1. Sixteen additional interspecific crosses from other, incomplete, crossing series (ALCH4X × BARK, ALCH4X × FRUT, ALCH4X × YEME, ARID × QUIN, FRUT × ACET, FRUT × BARK, INQU × TONG, PELT × ACET, PELT × ALCH, PELT × QUIN, QUIN × ARID, TONG × ACET, YEME × ALCH4X, ZONA × MULT, ZONA × QUIN) were also analyzed. We used embryo rescue (ER) of all F_1's to maximize the number of offspring for evaluation of chlorosis phenotypes, thus eliminating hybrid incompatibilities caused by failures of endosperm development in normal seed development in the plant.

Assessing phenotypic effects of CNI

Phenotypes reflecting severity of plastome-induced CNI ('pCNI') are listed in Tables 2 and 3. They are distinguished here according to the following syndromes: I) 'green'—no virescence or chlorosis observed; II) 'near green'—virescence occurs under extreme physiological conditions; III) 'mildly chlorotic' —plants were always chlorotic, but never lethal; IV) 'severely chlorotic'—plants were always chlorotic and easily turned yellow or lethal; and V) 'lethal'—plants were always yellow or white. In the case of uniparental inheritance of organelles, the correlation of phenotype with genotype is straightforward. In an equal F_1 nuclear genomic background, a direct connection can be established between the observed pCNI phenotype and the 'responsible' chloroplast genotype in an F_1. In the case of variegated offspring, which we suspected contained chloroplasts inherited from both parents, we tested, when possible, green and white parts of leaves separately.

Flow cytometry

The average total genomic content per cell (2C value expressed in pg) was determined using flow cytometry (Iribov SBW, the Netherlands) for all 19 accessions. As a reference for the size estimates, we used *P.* × *hortorum* PEZ-BD8517 with known ploidy (2×) and total genome size (2C = 2.33 pg). The measurements were done on freshly collected leaf material using a Partec CA-II flow-cytometer (De Laat et al. 1987). Nuclei were stained with a High-Resolution Kit (Partec).

Fig. 1 Experimental setup for the four comprehensive *Ciconium* crossing experiments. The four species indicated on the left were selected as mother plants. The *P.* × *hortorum* series is from Breman et al. (2020). The paternal accessions are listed to the right and their respective floral and leaf phenotypes are shown below the species names. The paternal accessions are arranged according to decreasing phylogenetic distances relative to *P.* × *hortorum* based on a repeatome-based phylogenetic analysis by Breman et al. (2021). The empty black squares indicate the mother plant in the series

Table 2 Categories of pCNI

	pCNI in F_1 offspring
I	green
II	green virescent
III	mildly affected; never fully green, but otherwise fine
IV	severely affected, always light green to yellow
V	lethal, white

Plastome assembly

Plastomes were assembled using GetOrganelle (Jin et al. 2019) using default settings, except for the assumed insert size which we set to 350. Contigs were visualized and assessed using Bandage (Wick et al. 2015) and final contigs were concatenated using MEGA7 (Kumar et al. 2016) and subsequently aligned in a multiple sequence alignment (MSA) with all accessions, using MAFFT (Katoh et al. 2019).

Organellar genotyping using PCR markers

We used diagnostic PCR to genotype the inherited chloroplasts following the methods and primers developed in the past research (Breman et al. 2020) with the aim of tracking the types of plastome inherited across the generations.

Ciconium rpo sequence variation

We assessed sequence variation in *rpoB*, *rpoC1* and *rpoC2* genes and in case we encountered length variation (>5 aa residues) in exons we explored its functional relevance by checking codons, translating the sequence to amino acids and determining physico-chemical properties for the inferred peptides (Table 4). The R-package 'Peptides' (Osorio et al. 2015) was used to calculate the weight (Da), grand average of hydrophobicity (GRAVY) index, aliphatic index ('aI'), iso-electric point of zero charge ('IEPoZC') (pH) and net charge at pH 7 (C) of

Table 3 Summary genotypes and phenotypes of F_1 interspecific crosses from *Pelargonium* section *Ciconium*

hybrid[a]	count	n/o plants tested	mCNI class	pCNI class maternal	pCNI class paternal	count of F_1 plastid types per plant maternal / paternal /biparental	chlorotic phenotypes[b]	other phenotype remarks
ACET **x** FRUT	3	3	II	I	I	0/1/2	C,G,V	
ACET **x** INQU	5	1	II	-	I	0/1/0	G	
ACET **x** ZONA	>20	9	V	-	V	0/7/2	C,V,+	
BARK **x** FRUT	4	4	IV	IV	-	4/0/0	C,G	small*, weak plant
BARK **x** INQU	2	2	V	?	?	0/2/0	G,+	died after seedling phase
BARK **x** MULT	10	3	III	III	III	0/2/1	V,C	Small plants
BARK **x** QUIN	2	2	V	IV	IV	1/0/1	C,V,L,+	Plantlet only
MULT **x** ACET	2	2	V	IV	IV	1/0/2	C,V	small, weak plant
MULT **x** ALCH	>20	13	II[d,e]	I	I	8/3/3	C,G,V	Often large
MULT **x** ARID	>20	3	III	I	-	3/0/0	C,G,V	one dwarf plant
MULT **x** BARK	10	6	III	III	III	6/0/1	C,V	Small plants
MULT **x** PELT	2	2	III	III	II	0/0/2	C,V	
MULT **x** QUIN	10	6	II[d,e]	?	?	-/-/-	G	Large
MULT **x** RANU	10	9	II[d,e]	I	I	1/7/1	C,G,V	Large
MULT **x** ZONA	1	1	V	IV	-	1/0/0	C	small, weak plant
ALCH4X **x** BARK	2	2	IV	II	-	2/0/0	G,V	
ALCH4X **x** FRUT	2	2	IV	II	III	1/0/0	C	Small
ALCH4X **x** YEME	3	3	III-II[p6]	I	I	2/1/0	C,G,V	
ARID **x** QUIN	>20	3	IV[c]	II	-	3/0/0	C,G	Often large plants
FRUT **x** ACET	5	1	I-II	I	I	0/0/1	G	fertile pollen
FRUT **x** BARK	6	6	IV[c]	III	III	5/0/1	C	small, weak plant
INQU **x** TONG	3	1	V	III	-	1/0/0	C	
PELT **x** ACET	4	4	IV	II	II	2/0/2	C,V	Small
PELT **x** ALCH	2	2	V	I	-	2/0/0	G	Very small
PELT **x** QUIN	1	1	V	-	III	0/1/0	C	small, weak plant
QUIN **x** ARID	10	3	IV[c]	II	-	3/0/0	C,G	Reciprocals equal
TONG **x** ACET	7	7	III	II	II	6/0/1	G	
YEME **x** ALCH4X	>20	1	I-II	I	-	1/0/0	G	
ZONA **x** MULT	1	1	V	III	III	0/0/1	C	small, weak plant
ZONA **x** QUIN	15	6	IV[c]	II	?	6/0/0	C,G	Often large

[a] maternal × paternal; *'Small' or 'large' indicates F_1 smaller/larger throughout life than either parent

[b] chlorotic phenotypes: *C* chlorotic, *G* green, *L* lethal seedlings, *V* variegation occurred, + = plant never made it past embryo rescue

[c] flowers only at temperature interval of 20-25°C

[d] fertility is temperature dependent 20-25°C

[e] not all individuals of these crosses displayed spontaneous seed set

[f] fertility only for polyploid, estimated level indicated

each amino acid sequence, over both the full-length exon and the variable regions.

Three-dimensional (3D) homology models of *Ciconium* rpoB and rpoC1 were generated using the SWISS-MODEL protein homology modeling server (Bertoni et al. 2017; Bienert et al. 2017; Waterhouse et al. 2018; Studer et al. 2020, 2021). As a template, we used the crystal structure of *Thermus thermophilus* transcription initiation complex (TIC) (PDB ID: 4g7h, Zhang et al. 2012) which is the PEP bacterial homolog.

The PyMOL software (https://www.pymol.org/) was used to visualize the 3D homology model, compare it to the *T. thermophilus* transcription initiation complex, calculate distances, and prepare Figs. 4 and 5. The quality of the homology models was assessed using the GMQE and QMEAN scoring functions (Biasini et al. 2014).

Correlation of phenotype with rpo types

The correlation (R^2) between rpo genotypes and observed leaf phenotypes was assessed by performing a linear

Table 4 rpoB peptide physico-chemical properties of the aa sequence across the full length

Accession	length (aa[a])	weight (Da)	gravy[b]	aliphatic index	Iso-electric point of zero charge (pH)	net charge (C) (at pH 7)
HOSA	1079,000	122558,304	-0,278	91,536	9,197	20,624
INQU	1079,000	122516,223	-0,282	91,273	9,197	20,624
FRUT	1079,000	122558,261	-0,277	91,536	9,140	19,625
ACET	1079,000	122602,228	-0,298	90,209	9,258	21,536
ACRA	1083,000	123144,691	-0,299	91,445	8,429	9,639
ZONA	1081,000	122795,291	-0,283	91,982	8,510	10,636
TONG	1085,000	123420,939	-0,293	91,891	8,165	6,641
MUYE	1085,000	123330,699	-0,294	91,627	7,958	4,546
OMAN	1085,000	123381,859	-0,288	91,627	8,253	7,544
INSU	1085,000	123333,771	-0,291	91,627	8,162	6,546
QUSO	1085,000	123333,771	-0,291	91,627	8,162	6,546
PELT	1081,000	122735,350	-0,293	90,827	9,010	17,538
RANU	1085,000	123338,707	-0,287	91,364	8,064	5,548
ALCH4X	1087,000	123610,067	-0,293	91,364	8,162	6,549
ALCH2X	1089,000	123818,194	-0,293	91,364	7,957	4,549
BARK	1084,000	123014,678	-0,276	93,309	8,736	13,449
ARTI	1081,000	122640,197	-0,267	92,691	8,587	11,632
ARID	1088,000	123766,202	-0,288	91,536	7,956	4,548
ELON	1077,000	122135,299	-0,284	91,536	8,378	8,601

[a] amino acid residues

[b] grand average of hydrophobicity

regression on the differences between four physico-chemical properties of the rpo aa-sequences of each accession and the observed paternal/maternal phenotypes in each F_1 cross. The four properties analyzed are: Gravy, aI, IEPoZC and net charge at C. The analyses were performed on rpoB and rpoC1 separately as well as on rpoB+CI for the two most complete series of crossings (the F_1's of *P.* × *hortorum* X *Ciconium* series and of the *P. multibracteatum* × *Ciconium* crossing series). The results are listed in Table 3.

Results

Confirmed F_1 hybrids

To compare the effects of different chloroplasts on chlorosis, we created a total of 30 verified F_1 interspecific hybrids (see Table 3) over four crossing seasons, by crossing *P. acetosum*, *P. barklyi* and *P. multibracteatum* with all other available *Ciconium* species. In addition, there were crossings available from our previous study (Breman et al. 2020) involving *P.* × *hortorum* as well as the genotypes for each offspring from that study. Using embryo rescue, we obtained offspring for nearly all interspecific crosses for which fruit and seed set was observed and we observed all modes of plastid inheritance (*i.e.* paternal, maternal and biparental) (Table 3). In most cases, at least some individuals of an offspring died quickly after germination or transplantation to the greenhouse. This was especially the case for MULT × ZONA, MULT × ACET, ACET × ZONA and BARK × QUIN from which a maximum of one, but usually no plants at all, survived transplantation to the greenhouse.

For the *P. acetosum* series, we obtained six F_1 interspecific hybrids (see Table 3). Two were from reciprocal crosses (MULT × ACET and PELT × ACET) and these were chlorotic and sterile (pCNI class III). Progeny of cross ACET × ZONA was always lethal (pNCI and mCNI class V), as the plants never flowered. ACET × TONG, ACET, × FRUT and ACET × INQU yielded plants that were green or near green and were partially male-fertile (pCNI class II).

For the *P. barklyi* series, we obtained four verified F_1 plants (BARK × FRUT, BARK × MULT, and BARK × QUIN). For BARK × INQU, we were unable to verify the status based on phenotype and it will not be considered further here. The three remaining crosses were chlorotic and sterile dwarfs (pCNI class III). Four more were obtained from reciprocal crosses (FRUT × BARK, MULT × BARK, HORT × BARK, ALCH4x × BARK). In addition, BARK × HORT was lethal as the plant was white, did not survive outside the laboratory and never flowered (pCNI class V). Two plants (BARK × MULT, and ALCH4x × BARK) were chlorotic and infertile (pCNI class III). One (BARK × FRUT) was severely chlorotic and flowered only once with sterile flowers, and the plants were dwarfs (pCNI class IV).

For the *P. multibracteatum* series, we obtained eight F_1 hybrids (see Table 3). Two of these (MULT × ALCH, MULT × QUIN) were green or near green and partially fertile (pCNI class II). Two (F_1 MULT × ARID, MULT × BARK) were chlorotic and infertile (pCNI class III). Three were severely chlorotic and flowering was never observed (F_1 MULT × ACET and MULT × ZONA, pCNI IV, mCNI V). *Pelargonium multibracteatum* crosses with INQU, FRUT and TONG did not yield a single plant despite two full seasons of crossing attempts. Finally, *P. multibracteatum* crosses with ACET or ZONA rarely yielded progeny, and when they did the plants nearly always carried the MULT plastid. We found one case where the F_1 MULT × ACET also carried the ACET plastid, alongside that from MULT. From the other crosses we obtained a further 15 F_1's, using additional *Ciconium* species as parents. From these series, the crosses with *P. yemenense* sp. Nov or *P. alchemilloides* (4x) with other accessions (*P. barklyi* and *P. frutetorum*) stand out as they were performed using parental accessions with different ploidy levels, resulting in polyploid offspring (see Fig. 2). We found maternal, paternal and biparentally inherited plastids across all F_1 offspring (Table 3) and clear differences exist, in some cases, with respect to plastid type inherited and resulting chlorosis in the offspring. All chlorosis- and fertility-related phenotypes for the four crossing series are displayed in Table 5. All individual plants, together with their chlorosis phenotype, and plastid genotypes, are listed in Additional file 1 (see below).

Flow cytometry

In order to check for polyploidy, we performed flow cytometry on F_1 hybrids. The results show that F_1 hybrids have a C-value that is intermediate between the two parents (Fig. 2). The most striking result is the frequency of polyploids, especially for the MULT-series (Fig. 2) and the other crosses (see Additional file 1). We were unable to obtain flow cytometry readings for all verified hybrids because some of these never made it past the embryo rescue stage or died quickly after germination or transplantation to the greenhouse, which left us with insufficient material for analysis.

Plastome-typing

We performed PCR's to determine the plastome-types inherited, and our results indicated plastomes to be inherited from either parent (Table 2).

For the *P. multibracteatum* series the results were conflicting. The individual plant used to extract the DNA from and to assemble the plastome from did test correctly, but other individuals from the same *P. multibracteatum* donor population also contained a non-*multibracteatum* genotype.

Ciconium rpo sequence variation and physico-chemical properties

To determine the level and type of variation in *rpo* genes we aligned *rpoB*, *rpoC1* and *C2* sequences for all accessions. From this alignment we noted three regions

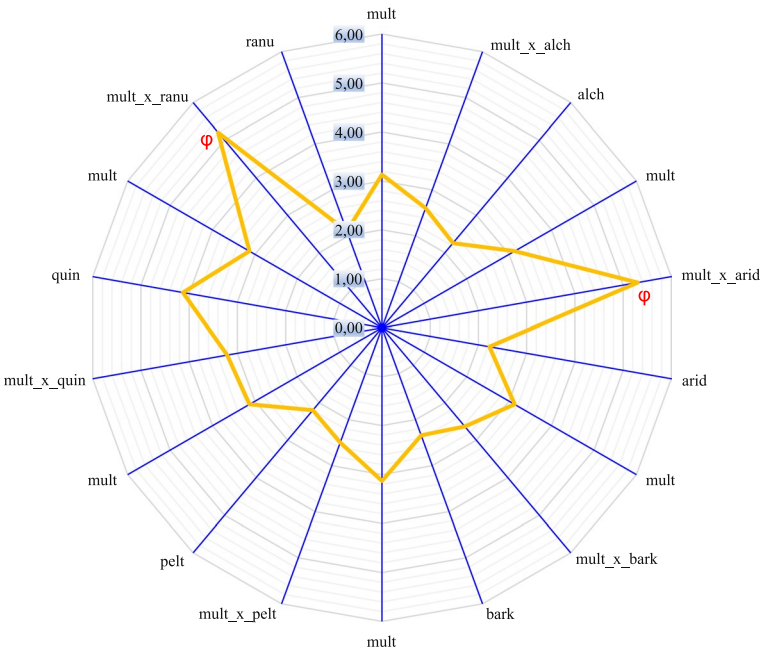

Fig. 2 Spiderweb diagram displaying Cx-values for the F_1 *Pelargonium multibracteatum* crossing series showing parental and F_1 hybrid genome sizes. The vertical axis displays the obtained Cx-values. The polyploids are indicated with **φ**. Species and accessions are more or less phylogenetically arranged. Two parental species flank each F_1 hybrid (*i.e.*, a *P. multibracteatum* parent crossed with another species from *P.* sect *Ciconium*)

Table 5 Correlation of phenotype and *rpo* physico-chemical properties by linear regression

	***Pelargonium* × *hortorum* series**							
	phenotype maternal				**phenotype paternal**			
	Δ gravy	**Δ aliphatic index**	**Δ IEPoZC (pH)**	**Δ net charge (at pH 7)**	**Δ gravy**	**Δ aliphatic index**	**Δ IEPoZC (pH)**	**Δ net charge (at pH 7)**
rpoB	0.5287	0.00548	0.5504	0.5726	0.00438	0.2582	0.3285	0.3627
rpoC1	0.2979	0.2871	0.5857	0.551	0.045	0.0864	0.0726	0.0475
rpoB + rpoC1	0.4996	0.1764	0.6198	0.6621	0.059	0.2573	0.2995	0.2573
	***P. multibracteatum* series**							
rpoB	0.083	0.1895	0.5393	0.1786	0.049	0.501	0.4958	0.4972
rpoC1	0.0149	0.1178	0.2413	0.1968	0.038	0.033	0.18	0.2251
rpoB + rpoC1	0.2159	0.16	0.2299	0.2446	0.2549	0.0602	0.5096	0.4821

containing significant variation (Fig. 3a-c), both in length as well as in amino acid composition. These 'variable indel' (*vind*) regions will be referred to as the '*rpoB*-vind', '*rpoC1*-vind1' and '*rpoC1*-vind2' regions. The alignment for *rpoC2*, showed length variation of one to three aa residues at nine different sites (not shown) and are not considered as 'vind' regions here.

A striking feature in the *Ciconium rpoB* genes is the occurrence of three aa insertions of threonine (T), aspartic acid (E) and tyrosine (Y) in various combinations. These 'TEY' motive insertions are largest in *P. aridum* (14 amino acids in total) and absent in *P. inquinans*, *P. acetosum*, *P.* × *hortorum*, *P.* × *salmoneum* and *P. frutetorum* (Fig. 3a) For rpoC1-vind1, insertions consist of serine (S) and guanine (G) in ZONA, ACRA and TONG (Fig. 3b). For rpoC1-vind2, length variation is caused by the insertion of E, T and arginine (R) at this site (Fig. 3c).

To assess what consequences these variations may have on protein function, we calculated some of their physicochemical properties: Da, GRAVY index, 'aI', 'IEPoZC' (pH) and net charge at C (Table 4). Across 20 *rpoB*- and C1 sequences the 'IEPoZC' and 'net-charge at pH 7', show the most striking differences between the accessions. The highest net charge for rpoB is for *P. acetosum* with a value of 21.5 C, and the lowest is for *P. aridum* (4.5 C), which has the second highest one for rpoC1 (40.8). a difference of 17.0 C. remarkably for these species the values for rpoC1 are exactly reversed. *P. acetosum* has the lowest value with 23.9 for rpoC1, whereas *P. aridum* has the second highest for rpoC1 (40.8). The (corresponding) isoelectric points differ the most for these two accessions as well, with the highest pH for *P. acetosum* for rpoB (pH 9.3) but the *P. acetosum* IEPoZC for rpoC1 is at pH 9.7 and this is the lowest from all accession, for *P. aridum* rpoB the IEPoZC is at pH 8.0 and for rpoC1 it is at pH 10.3.

The *P. acetosum* peptides were selected as examples of our modelling because of the high number of amino acid changes and presence of a large deletion in *rpoB* and a large insertion in *rpoC1* vind1 compared to other *Ciconium* species (Fig. 3a, b, c). The *T. thermophilus* rpoB and rpoC1 were identified as the best template available because these showed the highest sequence overlap (98.5% and 95.5%) and sequence identity (37.86% and 60%) with *P. acetosum* rpoB and rpoC1. For rpoC2, only partial templates covering the N-terminal part of the sequence were available (sequence overlap 28%, sequence identity 40.16%). Therefore, we could model the first 331 residues only. Based on that, all rpoC2 variants yielded a structurally similar model.

Structure modelling

The *P. acetosum* homology models (Figs. 4a, and 5a) for rpoB, rpoC1 and rpoC2 yielded qmean scores of -2.74, 0.63 and 0.45 and gmqe of 0.67, 0.53, and 0.16, respectively. The values for rpoB and rpoC1 are considered 'reasonable' in terms of reliability of the model but for rpoC2 they are low.

The 3D model of the *T. thermophilus* PEP (PDB ID: 4g7h) showed that the rpoB-vind, rpoC1-vind1 and rpoC1-vind2 regions are not in contact with the other operons but in close vicinity of the sigma factor (rpoC1-vind1) and template DNA/RNA (rpoB-vind and rpoC1-vind2) (Figs. 4d, e and 5c, d). Given the high qmean and gqme values for the bacterial and the *P. acetosum* rpoB and rpoC1 models, the general structure observed in the bacterial PEP is probably conserved in the *P. acetosum* PEP at least for these two regions.

The rpoB model showed a high structural similarity with its bacterial homologue, except for two unique features. The first one is a region that consists of three long helices in *T. thermophilus* but of two shorter helices in

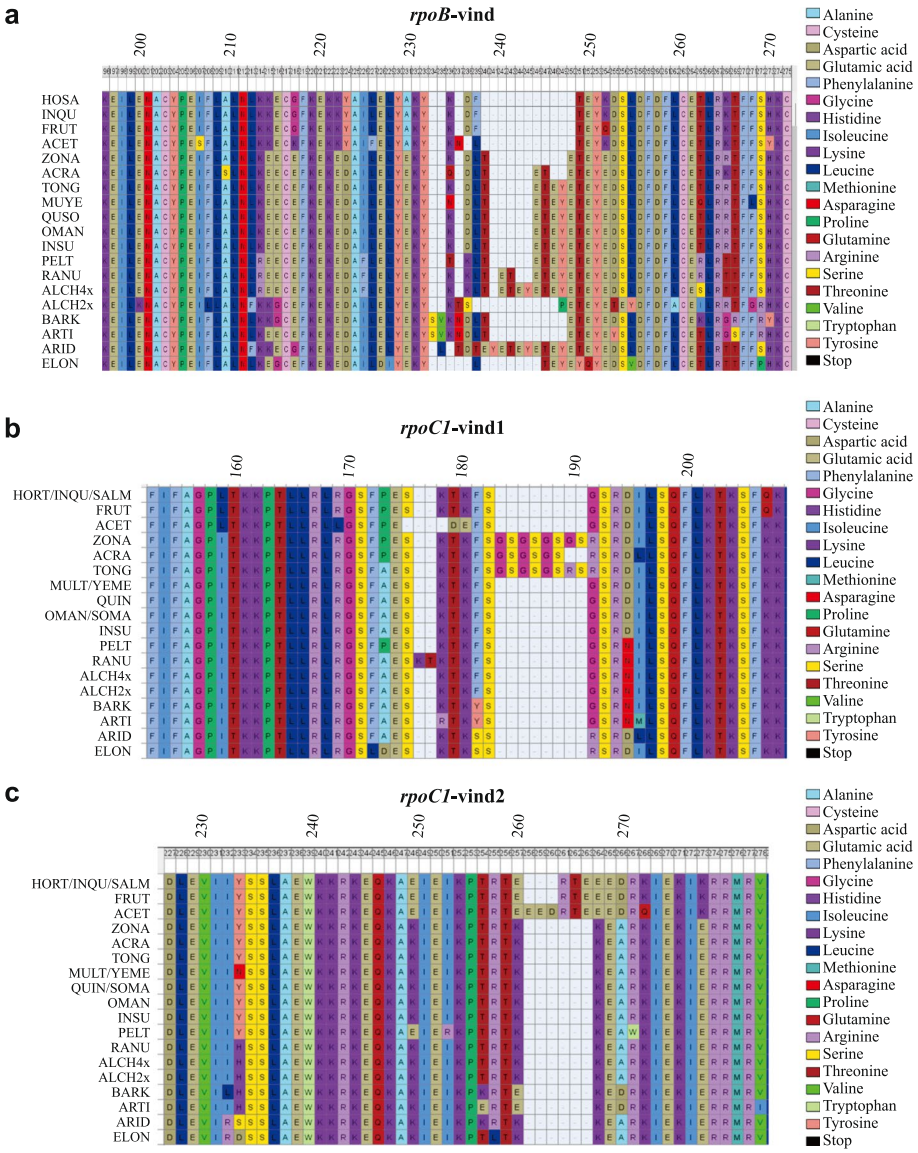

Fig. 3 Amino acid sequence alignment of *Ciconium rpo*-vind regions. *rpoB*-vind (**a**), *rpoC1*-vind1 (**b**) and *rpoC1*-vind2 (**c**). Numbering indicates amino acid position in the exon. Color codes for amino acids are listed at the right of the figure (a). The regions are flanked by non-length variable regions (not shown)

P. acetosum. In the *P. acetosum* rpoB model, this region is located at the extreme opposite of the *rpoB*-vind region (Fig. 4b) and will not be further discussed. The second one is the *rpoB*-vind region itself, where *Ciconium* either possesses a longer alpha helix or an unordered region, and near which *T. thermophilus* possesses a unique beta-sheet (Fig. 4b). According to this model, the *P. acetosum rpoB*-vind region consists of two alpha helices connected by an unordered region (Fig. 4c, d). In summary, our modelling of all *Ciconium* rpoB sequences resulted in four rpoB structural variants (Fig. 4a, b, c, d, e): structure a was observed for ELON, ACET, FRUT, INQU, SALM and HORT; structure b for ALCH2x & 4x, ARID, BARK, INSU, OMAN, QUIN, SOMA and ZONA; structure c for MULT,YEME, RANU, ARTI, ACRA and TONG; and structure d for PELT only.

Similarly, for rpoC1, three regions are variable between the plant and bacterial models. One is a region far removed from the *rpoC1*-vind1 and 2 regions (not shown), where the plant protein contains two alpha helices, whereas the bacterial model has two beta sheets. The other two are the *rpoC1*-vind1 and 2 regions (see Fig. 5). Modelling of these regions for all *Ciconium* sequences revealed that *rpoC1*-vind1 region is defined

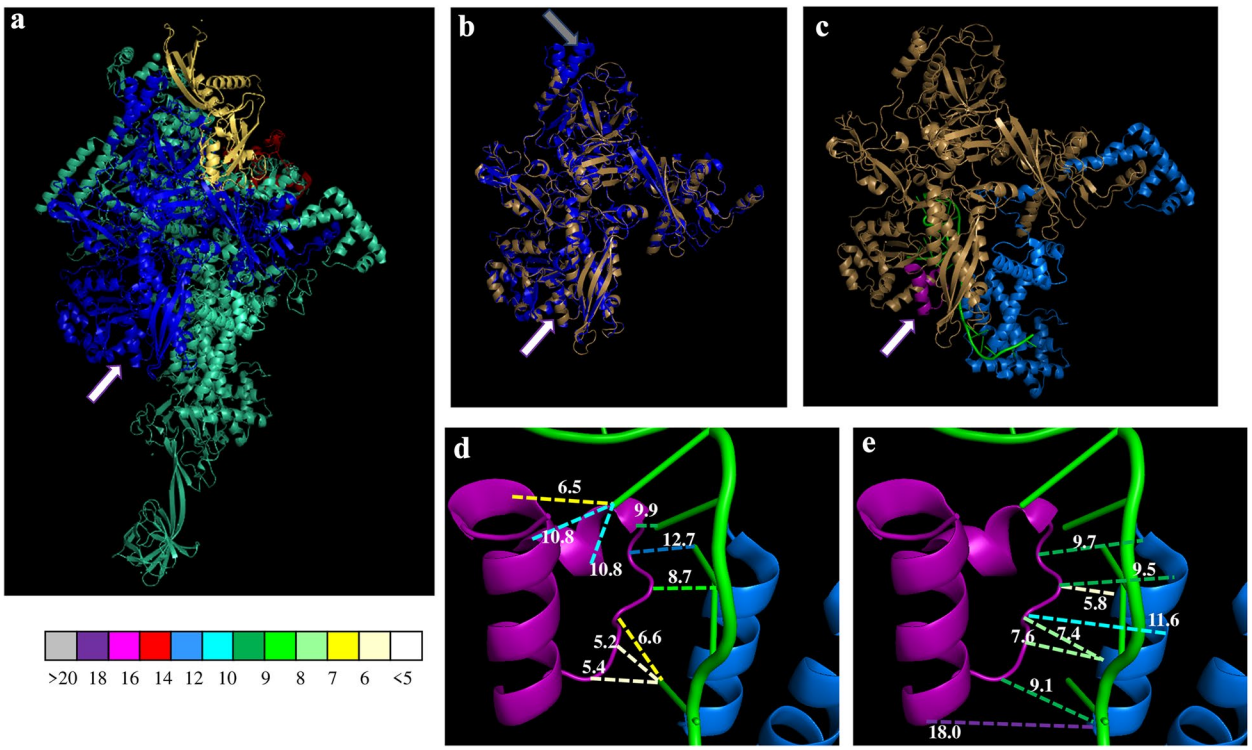

Fig. 4 *Thermus thermophilus* Transcription Initiation Complex (TIC, PDB ID: 4g7h) and 3D homology model of *Pelargonium* acetosum rpoB. (**a**) The full *T. thermophilus* Transcription Initiation operon. The four separately encoded parts are indicated with colouring, with yellow denoting subunit α, blue subunit β, teal the subunit β′ and red subunit β″ (although this is encoded in a single gene in the bacterial model with β′). The white arrow indicates the *rpoB*-vind homologue; (**b**) The plastid-encoded RNA polymerase (PEP) β subunit overlayed with the *P. acetosum* model in gold. Arrows indicate unique regions for the bacterial model when compared to *P. acetosum* (grey arrow) and the *rpoB*-vind region (white arrow); (**c**) the *P. acetosum* PEP β subunit with the *rpoB*-vind region indicated in purple (and white arrow), template RNA indicated in green and the sigma factor in light blue; (**d**/**e**) zoom-in on the *P. acetosum* PEP β subunit region of interest (ROI) and the distances (in Å) of interaction between template ROI and RNA/sigma factor I (based on the bacterial model). Distances >20Å not indicated. Line colors correspond to the colors on the scale

by two types of unordered regions, *i.e.* a long and short one, as a direct result of the sequence length variation. *rpoC1*-vind2 modelling resulted in three alternative structures, defined by containing a single loop alpha helix flanked by two unordered regions INQU, HORT, SALM and FRUT, containing two short beta sheets (ACET only) and the majority is modelled to contain an unordered region at this site (all other accessions). For details see Additional file 2.

In our homology-based model the distances between the *rpoB/C1*-vind regions and the α factor/template DNA/RNA would range from 6-10 Å for *rpoB* (Fig. 4d), 12-18 Å for *rpoC1-vind1* (Fig. 5c) and 11-14 Å for *rpoC1-vind2* (Fig. 5d).

Besides rpoB, and rpoC1, the PEP complex in plants consists of two more fragments: rpoA and rpoC2 (or α and β). The gene(s) encoding *rpoA* is located in the repeat-rich region of the *Pelargonium* plastome and could not be assembled (Ruhlman et al. 2018). For *rpoC2* the (low) sequence variation is discussed above.

Correlation of leaf phenotype with *rpo* types

There is no strong correlation between the observed phenotype in a cross and the physico-chemical properties of the rpoB and rpoC1 peptides (see Table 5). The maximum correlation was found for the differences of netto charges (R^2 0.66) and for the IEPoZC (R^2 0.61) in the *P.* × *hortorum* crossing series for rpoB and rpoC1 sequences combined. For the MULT series correlation was highest in the IEPoZC and net charge. For the IEPoZC in the MULT series, it was highest when rpoB and C1 were combined (R^2 0.5096). the R^2 for the net charge was highest for the rpoB peptide (0.4972). All correlation values and graphs are displayed in supplementary materials (Additional file 3).

Discussion

To study *Ciconium* CNI in detail, we generated a total of 30 verified F_1 interspecific hybrids, over four crossing seasons. Given the high incidence with which nearly every wild species used in our study transmits plastids to

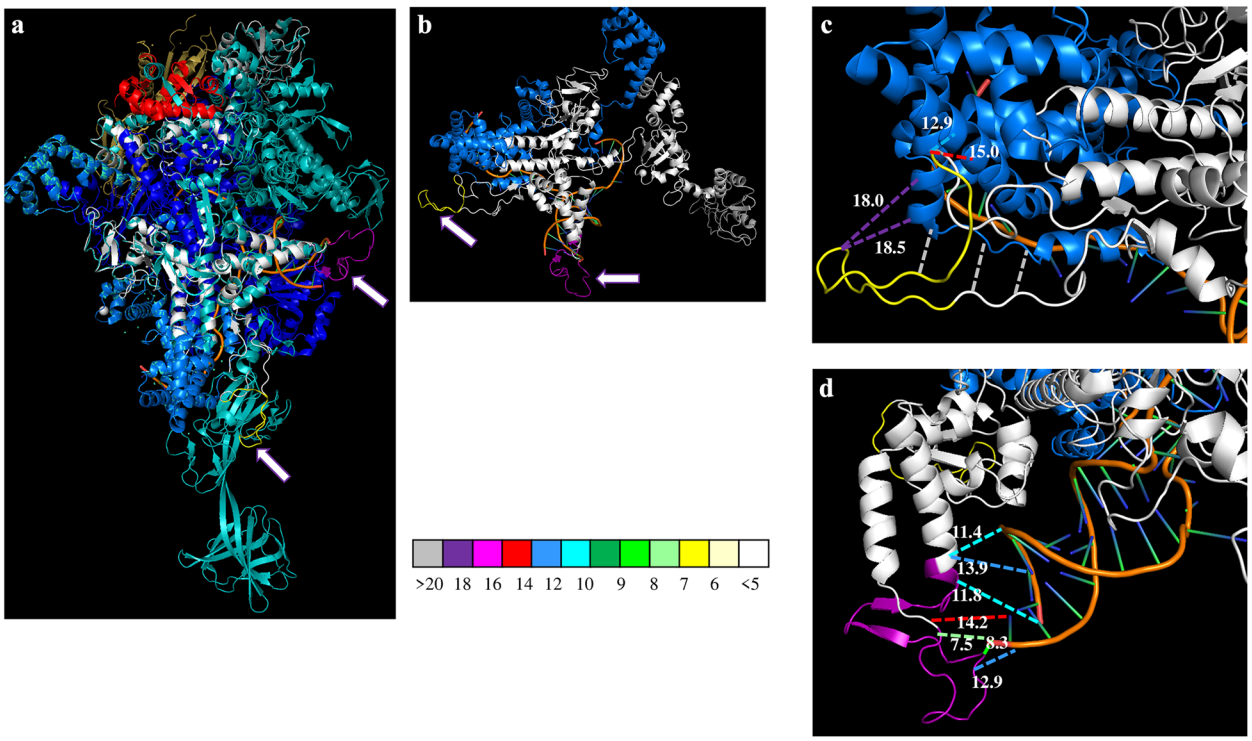

Fig. 5 *rpoC1*-vind structural interactions with DNA/RNA and σ-factor. (**a**) The full *Thermus. thermophilus* transcription initiation operon with the *P. acetosum* model overlayed; The four separately encoded parts of the Translation Initiation (TI) operon are independently-colored with: Yellow denotes subunit α, blue denoting subunit β, teal denoting subunit β′ and red denoting subunit β″ (although this is encoded in one gene in the bacterial model with β′). The white arrows indicates rpoC1-vind unique structures. Template DNA/RNA in orange-green and the σ-factor in light blue. Estimated physical distances are in Å. **b**) The PEP β′ subunit overlayed with the *P. acetosum* model in white (bacterial part in grey, which in part consists of β″). Arrows indicate unique rpoC1-vind1 (yellow) and 2 (purple) regions for the Ciconium model; **c**) Zoom in on the *P. acetosum* PEP β′ subunit with the rpoC1-vind1 region in yellow **d**) Zoom in on the *P. acetosum* PEP β′ subunit rpoC1-vind2 region of interaction between template ROI and RNA/sigma factor (based on the bacterial model)

the next generation, we conclude that biparental inheritance of chloroplasts occurs widely in *Ciconium* and that this is a property of the parent species, not an artifact of hybridization (Tilney-Basset et al. 1984, 1989a; Breman et al. 2020). We then explored the highly variable *Pelargonium* sect. *Ciconium rpo* gene and PEP protein structure and found that its sequence variation (which is actually higher than that found across angiosperms) leads to protein structural variation. We hypothesize that PEP structural variation in *P.* sect *Ciconium* results in evolutionary unstable structures which in turn may result in, possibly, a more error prone process of transcription. We modelled the PEP structures as they occur in *Ciconium* and found differences. The major structural differences we found to occur at sites that are in close contact with template dsDNA or processed ssRNA (Figs. 4, and 5). Of particular interest is the absence of an σ-helix or extended unordered region in the rpoB-vind region as well as the presence of an σ-helix in rpoC1-vind2 in the *P.* × *hortorum*/*inquinans*/*frutetorum* PEP structures. The plastomes of these species consistently lead to more lethality in our crossing series than any other plastome type. We hypothesize that not only PEP is evolutionary unstably, but it also has co-evolved with the nuclear encoded sigma factors (Zhang et al. 2013; Postel et al. 2022, for an example in *Silene*) and possibly with other nuclear encoded organelle management genes such as those encoding for PPR. To the point where the sigma factors from other species cannot interact properly with the different PEP subunits, thus leading to impaired function or even total cessation of development. The *P. acetosum* plastome is often lethal in crossings (its crossing series in our study were not successful), probably due to similar causes. The *P. acetosum* PEP also lacks the σ-helix or extended unordered region in the rpoB-vind and it, uniquely, contains two beta sheets in rpoC1-vind2 (Fig. 5d). The *P.* × *hortorum* crossing series was more successful in terms of established F_1 plants, probably because *P.* × *hortorum* is a hybrid plant itself which already went through several cycles of selection, among

others, for the ability to yield a green and robust plant. Further support for this comes from the fact that crosses with the main ancestor of *P.* × *hortorum* (*P. inquinans*) were also not that successful. Handling of template DNA/RNA by the PEP enzyme is dependent on refined and highly localized charge variations (Zhang et al. 2012; Sutherland and Murakami 2018). Local physico-chemical properties of one aa-change can already change the way DNA is entered into the PEP complex (or the way RNA is exported) and the *Ciconium* sequences have many. The fact that DNA/RNA handling sites appear to be affected may explain the occurrence of repeats and possibly also leads to selection pressure on promotor sites in the plastome (not shown).

We hypothesized that this variability might explain CNI as measured by chlorosis in *Pelargonium* F_1 interspecific hybrids. We reject the hypothesis that *rpo* gene variation alone can predict chlorosis in *P.* sect. *Ciconium* interspecific crosses. The correlations were at best ~ 60% (see Table 5 and further down).

Asymmetric inheritance due to lethal and non-lethal CNI

Chlorotic effects of different plastids on offspring are often asymmetric, meaning that reciprocal crossings differ usually in the transmission of pCNI to F_1 offspring. Furthermore, different chloroplast types induce different pCNI in crosses with equal nuclear genomic backgrounds. It is hard to explain the differences in chlorosis from F_1 hybrids when just considering the physico-chemical properties or sequences. If the nuclear genomic background is equal, why does one chloroplast type perform better in this background than another? Yet we sometimes see pronounced differences in phenotypes (*e.g.* the *P.* × hortorum/*P. inquinans* type chloroplast almost always causes a more chlorotic F_1 plant to occur when crossing. We therefore investigated the variation of the PEP protein structure in *P.* sect. *Ciconium* species.

Evolutionary unstable PEP structures in *P.* sect. *Ciconium*

Plastid encoded polymerase in plants is not well studied, often a bacterial model is assumed (*Escherichia. coli* or *T. thermophilus*) because of the chloroplasts' cyanobacterial origins (Cavalier-Smith 1982). Given the fact that three (rpoB or β, rpoC1 or β' and rpoC2 or γ) of the four plant subunits that make up PEP are homologues, this still allows us to deduce functional regions which may be affected by the changes. The rpoB1 and rpoC1 peptides are, when in the PEP complex, responsible for transcription. (Sutherland and Murakami 2018). As stated above, the variable regions of *Ciconium* PEP (and genus wide, Zhang et al. 2015) are located in regions of the subunits that are located near the uptake point where template dsDNA is taken into the enzyme (rpoC1-vind1) (Saecker et al. 2011; Sutherland and Murakami 2018). Here the unit interacts with the σ-factor and newly opened ssDNA (rpoB-vind see Fig. 4) (Saecker et al. 2011; Sutherland and Murakami 2018). Finally, rpoC1-vind2 is located near sites that interact with the σ-factor. We propose that, based on our modelling, PEP in *Pelargonium* affects the way template DNA is 'handled' during transcription and the way RNA is 'exported'.

The variants of PEP occurring may also differ in correcting mistakes or may produce slippage during transcription, and this may explain the abundance of repeat-rich regions in *Pelargonium* plastomes. Water availability, which is frequently limited in the natural area of *Ciconium* species, determines pH in the plant cells. This would lead to altered physico-chemical dynamics of the many proteins involved and therefore necessitate changes in the way the chloroplast is expressed because water is essential to photosynthesis. We hypothesize that the ubiquitous occurrence of biparental inheritance of chloroplasts is an evolutionary adaptation to 'cope' with the potential for high plastome variation brought on by the variation in the PEP enzyme (Although it could also be hypothesized the other way round; Robin van Velzen pers. comm.).

RpoA and rpoC2

rpoC2 is the part of the enzyme that is needed for the proper folding of the PEP complex (Igloi and Kussel 1992, Sutherland and Murakami 2018). Changes in the sequence for this gene may represent adjustments to the sequence changes in rpoB and rpoC1, ensuring a properly folded structure.

We were unable to reliably assemble rpoA from our Illumina data, as it is distributed among several contigs in the repeat-rich region of the plastome. It is still considered to form a functional part of the enzyme in *Pelargonium* (Blazier et al. 2016). In addition, rpoA does not have homologues in the bacterial model in terms of functionality. The plant rpoA subunit has derived so much from the bacterial ancestor that when transplanted into a bacterium, it was found to no longer function in the polymerase, whereas this is no problem for the other subunits (Suzuki and Maliga 2000). Given the high sequence variation in *Pelargonium* (Weng et al. 2016) and especially *Ciconium* rRNA sequences (compared to all other angiosperms, Breman et al. in prep.) we would suspect that rpoA is also highly variable and may contain structural variants as well. When attempting to use the few available sequences for *Ciconium* rpoA from GenBank, they all appear to be functioning operons (Blazier et al. 2016), but do not align well, neither at the nucleotide sequence nor the amino acid level. Further studies using long range

sequencing technologies should be conducted to get a better picture of rpoA gene structure.

Lack of correlation between phenotype and rpoB and rpoC1 physico-chemical properties

We have compared phenotypic effects versus two operons of one gene only, and could not find significant correlation (Table 5). While PEP is essential for gene expression in the chloroplast and appears to be under positive selection in *Ciconium* (Breman et al. 2021) it is not the only gene under positive selection (Breman et al. 2021a; Breman 2021b; Weng et al. 2016). Therefore, there may be other plastid encoded genes that are improperly expressed, such as uS19c or the genes encoding for ribosomal RNA (rrn23) as these are also highly diversified in *Ciconium* (Breman et al. 2021b). Given the critical importance of the ribosome for proper function of the chloroplast (Tiller et al. 2014 and references therein) the differences between the genes encoding for the various ribosomal elements (proteins and rRNA) may well also play a role in the occurrence of chlorosis in F_1 interspecific hybrids of *Ciconium*.

Another cause for the lack of correlation observed between leaf phenotypes and rpo may be that the peptides have more than one function. Part of the function is maintaining structure as well and may favor amino acid changes throughout the sequence. Given that our approach targets the entire sequence this may result in 'noise' from these other constraints.

The nuclear genomic perspective

Other factors also influence the expression and regulation of PEP and thereby also the chloroplast (Siniauskaya et al. 2016), which include the sigma (σ) factors (Zhang et al. 2015), *PPR* genes (Wang et al. 2021) and Whirly genes (Maréchal et al. 2009; Isemer et al. 2012). The *PPR* genes seem to be reduced in number in *P.* × *hortorum* when compared with other angiosperms (Zhang et al. 2013) and may be interesting candidates for further research in *Pelargonium* and CNI. Previous crossing experiments demonstrated clearly that nuclear genomic factors play a role in expression and regulation of chloroplasts (Tilney-Basset et al. 1989b, 1992; Breman et al. 2020) and these must be taken into consideration when studying CNI. The same holds for the 'interactome' (Westrich et al. 2021), which is the set of mainly nuclear-encoded proteins that fulfill numerous roles during assembly and maturation of PEP (Shikanai and Fujii 2013). Mitochondrial expression and regulation are managed by the nucleus as well, given the presence of mitochondrially target nuclear-encoded polymerases, but the extent of coevolution remains untested, at least for *Pelargonium*.

Our 3D homology model of *P. acetosum* rpo and its comparison with the *T. thermophilus* PEP allows for studying the rpo-vind regions in a broader context. Our comparisons seem to indicate that this region is located on the surface of the protein and interacts with both the target DNA and the σ-factor (Figs. 4 and 5). Substitutions, as well as the occurrence of indels in *Ciconium rpoB,* are reminiscent of what has been recorded for *Escherichia. coli* where it was demonstrated that changes in the transcription initiation (TI) complex may result in arrested transcription and subsequently to double-strand breaks (Dutta et al. 2011); although the exact nature of the change in the sequence may be different in plants when compared to the bacterial homologue. Nevertheless, the changes in *Ciconium rpoB* sequence may be affecting the 'cross-talk' between DNA repair, replication and transcription as well. Interestingly, the changes in the TI complex were found to be associated with changes in ribosomal activity in *E. coli* (Dutta et al. 2011), to compensate for changes in transcription speed.

Changes in cross-talk in addition to the previously detected changes in the replication, recombination and repair (RRR) machinery in Geraniaceae (Zhang et al. 2016), may partially explain the numerous indels and rearrangements found in the *Pelargonium* (and Geraniaceae) plastomes (Röschenbleck et al. 2017; Ruhlman et al. 2018). Especially changes that affect the transcriptional process are implicated in genomic disruption (Kim and Jinks-Robertson 2012; Sebastian and Oberdoerffer 2017) and should be considered in future studies of plastome evolution. Changes in the ribosomes of *Ciconium* were hypothesized to exist in the other research (Breman et al. 2021) in which the rRNA backbone was modelled of the large subunit and two ribosomal proteins.

Biparental inheritance of organelles and speciation

Plastids are undeveloped during and directly after fertilization and seed development, whereas the mitochondria are active during these phases. Thus, any mCNI effect would be stronger than pCNI at crucial early developmental stages. This would explain the high number of aborted embryos and empty seeds found on all our F_1 plants (not shown, but examples can be found in the reference, Breman et al. 2020). Given that the mother plant is 'responsible' for supplying energy to the development of the seeds, it is logical that there is a strong maternal bias. However, plastids are introduced to the embryo *via* pollen (Kuroiwa et al. 1992, 1993) and are sorted out, or expressed/developed incompletely in *Pelargonium*, early in development (Kirk and Tilney-Bassett 1967; Weihe

et al. 2009). Thus, they can be present in all tissues early in development (Guo and Hu 1995). Whereas mCNI hardly plays a role in the post seedling phase of the plant pCNI is considered to determine further survival during the vegetative phase of life. Our results lend support to the idea that biparental inheritance of organelles could provide an 'escape' from CNI (Barnard-Kubow et al. 2017). They also support the hypothesis that organellar changes, resulting in CNI, have a profound influence on speciation (Greiner et al. 2013; Barnard-Kubow et al. 2016). Further support for these two hypotheses comes from the fact that second generation of plants segregate again for chlorosis with only one plastid type present, showing that selection for organelle management and expression genes acts immediately after the first generation of hybridization (Barnard-Kubow et al. 2016; Breman et al. 2020).

Possible effects of bi-parental transmission on phylogeny reconstruction

The preference for one type, as well as preferentially backcrossing with one of the parents (introgression) after a historical hybridization event, could explain the problematic position of taxa in *Pelargonium* phylogenetic trees due to conflict between plastid and nuclear genomic markers. For instance, the four-petalled Clade A species *P. nanum,* which is currently not assigned to a section (Röschenbleck et al. 2014), was suspected to be an ancient hybrid species because of the unique floral morphology and its 'single branch' status in current phylogenies (van de Kerke et al. 2019). It was found to be sister to clade A2 (Bakker et al. 1999) and its inclusion in a Bayesian phylogeny reconstruction appeared to prevent the Markov Chains used from converging (Jones et al. 2008). Other cases can be seen in *P.* sect. *Hoarea* where the occurrence of 'non-monophyletic species' has been attributed to 'chloroplast capture' (Bakker et al. 2005). Such taxa would have retained the chloroplast of one species, while displaying the morphology and nuclear genomic type of another. Further testing of such incongruencies could be done by using more markers from the nuclear genomes. For instance, the repeatome appears promising as a source of phylogenetic markers (Dodsworth et al. 2015; Vitales et al. 2020; Breman et al. 2021) as it provides resolution at a low taxonomic level and provides a genome-wide overview represented by the most abundant parts of the non-coding DNA (repeats). Naturally occurring hybrids in *Pelargonium* are rarely found (pers. comm. Powrie, Kirstenbosch RSA), but not unheard off (Knuth et al. 1912, van der Walt et al. 1990). This is logical given the reduced fitness characteristic of most hybrid offspring which will result in lower chances of surviving to the reproductive life stage, as is supported by results from our experiments. However, our study also shows that species are highly compatible as we obtained many (~30) interspecific crosses, some of which produce fully green and fertile offspring. We therefore do not exclude that hybridization plays an additional, minor role in *Pelargonium* speciation (see above for *P. nanum*, and the allopolyploids *P. quercetorum, P. endlicherianum* and possibly *P. caylae* from Madagascar which could represent a hybrid species). Two cases of possible natural hybrids from *P.* section *Ciconium* are known. The first is an herbarium specimen of a wild hybrid between *P. peltatum* and *P. alchemilloides* at RBGE (M. Gibby pers. comm., FCB pers. observ.), the second case is *P.* × *salmoneum* (from our own collections). The morphology of *P.* × *salmoneum* is intermediate between the hypothesized parental species. The phylogenetic position based on the repeatome is also intermediate between the supposed parents. (Breman et al. 2021). *Pelargonium* × *salmoneum* is a fully fertile, green plant that segregates for numerous traits such as plant size, flower and leaf shape, indicating it is not a 'stable' species (yet), but a hybrid. We propose that *P.* × *salmoneum*, irrespective of whether it arose naturally or was the result of human crossing activities, is a genuine interspecific hybrid with equal fitness comparable to either of its proposed parents.

Other examples of chlorosis linked to *rpo* types

Few other examples of where *rpo* genotypes used to explain chlorosis in F_1 interspecific hybrids exist, but in *Zantedeschia,* for which recently four plastomes became available (He et al. 2020), when comparing the *rpo* types and known occurrence of chlorosis of interspecific crosses (RCS pers. obs.), we find that there is also an increase of chlorotic phenotypes with increased physicochemical distance. Interestingly *Zantedesschia* shares a number of characters with *Pelargonium*. Its species are relatively easy to cross (RCS pers. comm.), it has biparental inheritance of plastids (Yao et al. 1994) and nuclear genomic alleles have been implicated in explaining the observed patterns of chlorosis in the interspecific crosses as well (Yao et al. 2000, Snijder et al. 2007).

Conclusions

With current efforts underway to control photosynthesis more precisely (Teeuwen et al. 2022), the function PEP plays in chloroplast expression cannot be ignored. Knowledge of structural variants of PEP and their functional impact in the plastid environment may contribute to engineer PEP to function under different conditions such as heat/water stress.

Supplementary Information

The online version contains supplementary material available at https://doi.org/10.1007/s44281-023-00015-2.

Additional file 1: Table S1. Plastid genotypes for all crosses in this study. **Table S2.** Flow cytometry values obtained for all plants used in this study.

Additional file 2: Fig. S1. Structure models for rpo variable indel ('vind') regions including rpoB-vind (a-e), rpoC1-vind1 (f-g), rpoC1-vind2 (g-j). All were modelled using the bacterial homolog Thermus thermophilus transcription initiation complex (TIC) (PDB ID: 4g7h) as template. Explanation (**e**) of codes used for labelling structural elements, with 'α' indicating alpha helix and 'υ' indicating unordered regions (see text). Numbering immediately adjacent to α, β and υ indicates homologous element across all variants compared, and small black numbering indicates amino acid residue position. (**a**) rpoB υ4 is short, α5 is absent, occurs in ELON, ACET, FRUT, INQU, SALM, and HORT; (**b**) υ4 is elongated, α5 is absent, occurs in ALCH 2x and 4x, ARID, BARK, INSU, OMAN, QUIN, SOMA, and ZONA); (**c**) υ4 is interrupted by α5, occurs in MULT, YEME, RANU, ARTI, ACRA, and TONG; (**d**) υ4 is intermediate in length, α5 has fewer than 1 coil, occurs in PELT; (**f**) rpoC1-vind 'short', occurs in ELON, FRUT, INQU, SALM, HORT, ALCH 2x and 4x, ARID, BARK, INSU, OMAN, QUIN, SOMA, MULT, YEME, RANU, ARTI, and PELT; (**g**) rpoC1-vind1 'long', occurs in ACRA, TONG, and ZONA; (**h**) rpoC1-vind2 non-structured type, occurs in ELON, ACLH 2x and 4x, ARID, BARK, INSU, OMAN, QUIN, SOMA, MULT, YEME, RANU, ARTI, and PELT; (**i**) rpoC1-vind2 type with two beta sheets (indicated by 'β1' and 'β2'), occurs in ACET; and (**j**) rpoC1-vind2 type with one alpha helix α1, occurs in FRUT, INQU, SALM, and HORT.

Additional file 3: Table S3. Fig S2. Correlations between chlorosis phenotypes (see Table 2) and Physico-chemical properties of rpo peptides.

Acknowledgements
We appreciate the crews at Syngenta Enkhuizen (Nl) and Angers (F) for caring for the plants; Tony Lokkers (Syngenta) for pollinations; Mary Gibby, Sabrina Knees (RBGE) for valuable discussion on *Ciconium* species and sharing herbarium specimens and potentially new species; Justin van der Hooft (Wageningen University, Bioinformatics Group) for help with interpreting the structural peptide models and understanding the physicochemical properties. We also like to thank Jian Jun Jin for help with GetOrganelle.

Authors' contributions
Conceived the study: FCB, FTB, MES. Wrote the manuscript: FCB, FTB. Carried out the analysis: FCB. Peptide analysis FCB, CV. Experimental design PCR: FCB, FTB, *rpo* typing: FCB, FTB. Experimental design crossing and embryo rescue: FCB, RCS, MES, MS-S. Experimental design PCR: FCB, JWK. Laboratory work: FCB, JWK. All authors read the draft and gave feedback.

Funding
This research was funded by the Dutch Foundations for Applied Scientific Research (TTW), Grant number: 14531, "*Pelargoniumgenomics for overcoming cytonuclear incompatibility and bridging species barriers" of the Green Genetics program.*

Availability of data and materials
The datasets generated and/or analysed during the current study are available from the corresponding author on reasonable request.

Declarations

Ethics approval and consent to participate
Not applicable.

Consent for publication
Not applicable.

Competing interests
The authors declare that they have no competing interests. Prof. M. Eric Schranz is an editorial board member of *Horticulture Advances* and was not involved in the journal's review or decisions related to this manuscript.

Received: 8 June 2023 Revised: 26 September 2023 Accepted: 10 October 2023
Published online: 10 January 2024

References

Apitz J, Weihe A, Pohlheim F, Börner T. Biparental inheritance of organelles in *Pelargonium*: evidence for intergenomic recombination of mitochondrial DNA. Planta. 2013;237:509–15. https://doi.org/10.1007/s00425-012-1768-x.

Bakker FT, Hellbrügge D, Culjam A, Gibby M. Phylogenetic relationships within Pelargonium sect. Peristera (Geraniaceae) inferred from nrDNA and cpDNA sequence comparisons. Syst Evol. 1998;211:273–87. https://doi.org/10.1007/BF00985364.

Bakker FT, Culham A, Daugherty LC, Gibby M. A trnL-F based phylogeny for species of (Geraniaceae) with small chromosomes *Pelargonium*. Pl Syst Evol. 1999;216:309–24. https://doi.org/10.1007/BF01084405.

Bakker FT, Culham A, Hettiarachi P, Touloumenidou T, Gibby M. Phylogeny of *Pelargonium* (Geraniaceae) based on DNA sequences from three genomes. Taxon. 2004;53:17–28. https://doi.org/10.2307/4135485.

Bakker FT, Culham A, Marais EM, Gibby M. Nested radiation in cape *Pelargonium*. In: Bakker FT, Chartrou LW, Gravendeel B, Pielser PB, editors. Plant species-level systematics: new perspectives on pattern and process. A. R. G. Ganter Verlag K. G., Ruggell, Liechtstein. 2005. pp. 75–100.

Barnard-Kubow KB, So N, Galloway LF. Cytonuclear incompatibility contributes to the early stages of speciation. Evolution. 2016;70:2752–66. https://doi.org/10.1111/evo.13075.

Barnard-Kubow KB, McCoy MA, Galloway LF. Biparental chloroplast inheritance leads to rescue from cytonuclear incompatibility. New Phytol. 2017;213:1466–76. https://doi.org/10.1111/nph.14222.

Bateson W. Heredity and variation in modern lights. In: Seward AC, editor. Darwin and modern science. Cambridge, UK: Cambridge University Press; 1909. p. 85–101.

Baur E. Das Wesen und die Erblichkeitsverhältnisse der, Varietates albomarginatae hort. Von *Pelargonium* zonale . Z Ver-erbungslehre. 1909;1:330–51. https://doi.org/10.1007/BF01990603.

Bertoni M, Kiefer F, Biasini M, Bordoli L, Schwede T. Modeling protein quaternary structure of homo- and hetero-oligomers beyond binary interactions by homology. Sci Rep. 2017;7:10480. https://doi.org/10.1038/s41598-017-09654-8.

Biasini M, Bienert S, Waterhouse A, Arnold K, Studer G, Schmidt T, et al. SWISS-MODEL: modelling protein tertiary and quaternary structure using evolutionary information. Nucleic Acids Res. 2014;42:W252–8. https://doi.org/10.1093/nar/gku340.

Bienert S, Waterhouse A, de Beer TAP, Tauriello G, Studer G, Bordoli L, et al. The SWISS-MODEL repository – new features and functionality. Nucleic Acids Res. 2017;45:D313–9. https://doi.org/10.1093/nar/gkw1132.

Blazier JC, Ruhlman TA, Weng ML, Rehman SK, Sabir JSM, Jansen RK. Divergence of RNA polymerase a subunits in angiosperm plastid genomes is mediated by genomic rearrangement. Sci Rep. 2016;6(24):595. https://doi.org/10.1038/srep24595.

Börner T, Aleynikova AY, Zubo YO, Kusnetsov VV. Chloroplast RNA polymerases: role in chloroplast biogenesis. BBA. 2015;1847:761–9. https://doi.org/10.1016/j.bbabio.2015.02.004.

Breman FC, Snijder RC, Korver JW, Pelzer S, Sancho Such M, Schranz ME, et al. Interspecific hybrids between *Pelargonium* × *hortorum* and species from *P.* section *Ciconium* reveal biparental plastid inheritance and multi-locus cyto-nuclear incompatibility. Front Plant Sci. 2020;11:614871.

Breman FC, Schranz ME, Chen G, Snijder RC, Bakker FT. (2021a). Repeatome-based phylogenetics in Pelargonium section Ciconium (Sweet) Harvey. Genome Biology and Evolution evab269. https://doi.org/10.1093/gbe/evab269.

Breman FC. (2021b). Exploring patterns of cytonuclear incompatibility in Pelargonium section Ciconium. PhD thesis, Wageningen UR, the Netherlands. https://doi.org/10.18174/551565.
Breman FC, Schranz ME, Chen G, Snijder RC, Bakker FT. Repeatome-based phylogenetics in *Pelargonium* section *Ciconium* (Sweet) harvey. Genome Biol Evol. 2021;13:evab269. https://doi.org/10.1093/gbe/evab269.
Breman FC. Exploring patterns of cytonuclear incompatibility in *Pelargonium* section *Ciconium*. PhD thesis, Wageningen UR, the Netherlands. 2021. https://doi.org/10.18174/551565.
Canonge J, Roby C, Hamon C, Potin P, Pfannschmidt T, Philippot M. Occurrence of albinism during wheat androgenesis is correlated with repression of the key genes required for proper chloroplast biogenesis. Planta. 2021;254:123. https://doi.org/10.1007/s00425-021-03773-3.
Cavalier-Smith FLST. The origins of plastids. Biol J Linn Soc. 1982;17:289–306. https://doi.org/10.1111/j.1095-8312.1982.tb02023.x.
Chumley TW, Palmer JD, Mower JP, Fourcade MH, Calie PJ, Boore JL, et al. The complete chloroplast genome sequence of *Pelargonium* × *hortorum*: organization and evolution of the largest and most highly rearranged chloroplast genome of land plants. Mol Biol Evol. 2006;23:2175–90. https://doi.org/10.1093/molbev/msl089.
De Laat A, Godhe W, Vogelzang M. Determination of ploidy of single plants and populations by flow cytometry. Plant Breed. 1987;99:303–7. https://doi.org/10.1111/j.1439-0523.1987.tb01186.x.
Demarsy E, Courtois F, Azevedo J, Buhot L, Lerbs-Mache S. Building up of the plastid transcriptional machinery during germination and early plant development. Physiol. 2006;142:993–1003. https://doi.org/10.1104/pp.106.085043.
Dobzhansky T. Studies on hybrid sterility. II. Localization of sterility factors in *Drosophila pseudoobscura* hybrids. Genetics. 1936;21:113–35. https://doi.org/10.1093/genetics/21.2.113.
Dodsworth S, Chase MW, Kelly LJ, Leitch IJ, Macas J, et al. Genomic repeat abundances contain phylogenetic signal. Syst Biol. 2015;64:112–26. https://doi.org/10.1093/sysbio/syu080.
Dutta D, Shatalin K, Epshtein V, Gottesman ME, Nudler E. Linking RNA polymerase backtracking to genome instability in *E. coli*. Cell. 2011;146:533–43. https://doi.org/10.1016/j.cell.2011.07.034.
Forsythe ES, Williams AM, Sloan DB. Genome-wide signatures of plastid-nuclear coevolution point to repeated perturbations of plastid proteostasis systems across angiosperms. Plant Cell. 2021;33:980–97. https://doi.org/10.1093/plcell/koab021.
Greiner S, Rauwulf, U, Meurer J, Hermann RG. (2011). The role of plastids in plant speciation. Mol. Ecol. 20, 671–691. https://doi.org/10.1111/j.1365-294X.2010.04984.x.
Greiner S, Bock R. Tuning a ménage à trois: co-evolution and co-adaptation of nuclear and organellar genomes in plants. Bioessays. 2013;35:354–65. https://doi.org/10.1002/bies.201200137.
Greiner S, Sobanski J, Bock R. Why are most organelle genomes transmitted maternally? Bioessays. 2015;37:80–94. https://doi.org/10.1002/bies.201400110.
Guisinger MM, Kuehl JV, Boore JL, Jansen RK. Genome-wide analyses of *Geraniaceae* plastid DNA reveal unprecedented patterns of increased nucleotide substitutions. Proc Natl Acad. 2008;105:18424–9. https://doi.org/10.1073/pnas.0806759105.
Guo FL, Hu SY. Cytological evidence of biparental inheritance of plastids and mitochondria in *Pelargoniu*m. Protoplasma. 1995;186:201–7. https://doi.org/10.1007/BF01281330.
Harvey WH. Geraniaceae. In: Harvey WH, Sonder OW, editors. Flora capensis, vol. 1. Hodges, Smith & Co, Dublin; 1860. p. 259–308.
He S, Yang Y, Li Z, Wang X, Guo Y, Wu H. Comparative analysis of four *Zantedeschia* chloroplast genomes: expansion and contraction of the IR region, phylogenetic analyses and SSR genetic diversity assessment. PeerJ. 2020;8:e9132. https://doi.org/10.7717/peerj.9132.
Horn W. Interspecific crossability and inheritance in *Pelargonium*. Plant Breed. 1994;113:3–17. https://doi.org/10.1111/j.1439-0523.1994.tb00696.x.
Igloi GL, Kössel H. The transcriptional apparatus of chloroplasts. Crit Rev Plant Sci. 1992;10:525–58. https://doi.org/10.1080/07352689209382326.
Isemer R, Mulisch M, Schäfer A, Kirchner S, Koop HU, Krupinska K. Recombinant Whirly1 translocates from transplastomic chloroplasts to the nucleus. FEBS Letters. 2012;586:85–8. https://doi.org/10.1016/j.febslet.2011.11.029.
James CM, Gibby M, Barrett JA. Molecular studies in *Pelargonium* (Geraniaceae). A taxonomic appraisal of section *Ciconium* and the origin of the "Zonal" and "Ivy-leaved" cultivars. Plant Syst Evol. 2004;243:131–46. https://doi.org/10.1007/s00606-003-0074-2.
Jin JJ, Yu WB, Yang JB, Song Y, dePamphilis CW, Yi TS, et al. GetOrganelle: a fast and versatile toolkit for accurate de novo assembly of organelle genomes. bioRxiv. 2019; 256479. https://doi.org/10.1101/256479.
Jones CS, Bakker FT, Schlichting CD, Nicotra AB. Leaf shape evolution LEAF SHAPE EVOLUTION in the South African genus *Pelargonium* L'Hér (Geraniaceae). Evolution. 2009;63:479–97. https://doi.org/10.1111/j.1558-5646.2008.00552.x.
Katoh K, Rozewicki J, Yamada KD. MAFFT online service: multiple sequence alignment, interactive sequence choice and visualization. Brief Bioinform. 2019;20:1160–6. https://doi.org/10.1093/bib/bbx108.
Kim N, Jinks-Robertson S. Transcription as a source of genome instability. Nat Rev Genet. 2012;13:204–14. https://doi.org/10.1038/nrg3152.
Kirk JTO, Tilney-Bassett RAE. The plastids. London: Freeman and Co.; 1967.
Knuth R. Geraniaceae. In: Encler A, editor. Das Pflanzenreich 4. Leipzig: Engelmann; 1912. p. 1–9.
Kumar S, Stecher G, Tamura K. MEGA7: Molecular Evolutionary Genetics Analysis version 7.0 for bigger datasets. Mol Biol Evol. 2016;33:1870–4. https://doi.org/10.1093/molbev/msw054.
Kuroiwa H, Kuroiwa T. Giant mitochondria in the mature egg cell of *Pelargonium zonale*. Protoplasma. 1992;168:184–8. https://doi.org/10.1007/BF01666264.
Kuroiwa T, Kawazu T, Ushida H, Ohta T, Kuroiwa H. Direct evidence of plastid DNA and mitochondrial DNA in sperm cells in relation to biparental inheritance of organelle DNA in *Pelargonium zonale* by fluorescence/electron microscopy. Eur J Cell Biol. 1993;62:307–13.
Maréchal A, Parent JS, Véronneau-Lafortune F, Joyeux A, Lang BF, Brisson B. Whirly proteins maintain plastid genome stability in *Arabidopsis*. PNAS. 2009;106(34):14693–8. https://doi.org/10.1073/pnas.0901710106.
Metzlaff M, Börner T, Hagemann R. Variations of chloroplast DNAs in the genus *Pelargonium* and their biparental inheritance. Theor Appl Genet. 1981;60:37–41. https://doi.org/10.1007/BF00275175.
Müller HJ. Isolating mechanisms, evolution, and temperature. Biol Symp. 1942;6:71–125.
Osorio D, Rondon-Villarreal P, Torres R. Peptides: a package for data mining of antimicrobial peptides. The R Journal. 2015;7:4–14. https://doi.org/10.32614/RJ-2015-001.
Palomar VM, Jaksich S, Fujii S, Kucinski J, Wierzbicki AT. High-resolution map of plastid-encoded RNA polymerase binding patterns demonstrates a major role of transcription in chloroplast gene expression. Plant J. 2022;111:1139–51. https://doi.org/10.1111/tpj.15882.
Postel Z, Touzet P. Cytonuclear genetic incompatibilities in plant speciation. Plants. 2020;9:487. https://doi.org/10.3390/plants9040487.
Postel Z, Poux C, Gallina S, Varré J-S, Godé C, Schmitt E, et al. Reproductive isolation among lineages of *Silene nutans* (Caryophyllaceae): a potential involvement of plastid–nuclear incompatibilities. Mol Phylogenet Evol. 2022;169:107436. https://doi.org/10.1016/j.ympev.2022.107436.
Qin T, Zhao P, Sun J, Zhao Y, Zhang Y, Yang Q, et al. Research progress of PPR proteins in RNA editing, stress response, plant growth and development. Front Genet. 2021;12:765580. https://doi.org/10.3389/fgene.2021.765580.
Röschenbleck J, Wicke S, Weinl S, Kudla J, Müller KF. Genus-wide screening reveals four distinct types of structural plastid genome organization in *Pelargonium* (Geraniaceae). Genome Biol Evol. 2017;9:64–76. https://doi.org/10.1093/gbe/evw271.
Röschenbleck J, Albers F, Müller K, Weinl S, Kudla J. Phylogenetics, character evolution and a subgeneric revision of the genus *Pelargonium* (Geraniaceae). Phytotaxa. 2014;159:31–76. https://doi.org/10.11646/phytotaxa.159.2.1.
Ruhlman TA, Jansen RK. Aberration or analogy? The atypical plastomes of Geraniaceae. In: Chaw, S-M, Jansen RK, editors. Advances in Botanical Research 85: Plastid Genome Evolution. Elsevier, Amsterdam; 2018, pp. 223–62. https://doi.org/10.1016/bs.abr.2017.11.017
Saecker RM, Record TM Jr, deHaseth PL. Mechanism of bacterial transcription initiation: RNA polymerase – promoter binding, isomerization to initiation-competent open complexes, and initiation of RNA synthesis. J Mol Biol. 2011;412:754–71. https://doi.org/10.1016/j.jmb.2011.01.018.
Schnable PS, Wise RP. The molecular basis of cytoplasmic male sterility and fertility restoration. Trends Plant Sci. 1998;3:175–80. https://doi.org/10.1016/S1360-1385(98)01235-7.

Sebastian R, Oberdoerffer P. Transcription-associated events affecting genomic integrity. Philos Trans R Soc Lond B Biol Sci. 2017;372:20160288. https://doi.org/10.1098/rstb.2016.0288.
Sharbrough J, Conover JL, Gyorfy MF, Grover CE, Miller ER, Wendel JF, et al. Global patterns of subgenome evolution in organelle-targeted genes of six allotetraploid angiosperms. Mol Biol Evol. 2022;39(4):msac074. https://doi.org/10.1093/molbev/msac074.
Shikanai T, Fujii S. Function of PPR proteins in plastid gene expression. RNA Biology. 2013;9:1446–56. https://doi.org/10.4161/rna.25207.
Siniauskaya MG, Danilenko NG, Lukhanina NV, Shymkevich AM, Davydenko OG. Expression of the chloroplast genome: modern concepts and experimental approaches. Russ J Genet Appl Res. 2016;6:491–509. https://doi.org/10.1134/S2079059716050117.
Snijder RC, Brown FS, van Tuyl JM. The Role of plastome-genome incompatibility and biparental plastid inheritance in interspecific hybridization in the genus *Zantedeschia* (Araceae). Floriculture and Ornamental Biotechnology. 2007;1:150–7.
Studer G, Tauriello G, Bienert S, Biasini M, Johner N, Schwede T. ProMod3 – a versatile homology modelling toolbox. PLOS Comp Biol. 2021;17:e1008667. https://doi.org/10.1371/journal.pcbi.1008667.
Studer G, Rempfer C, Waterhouse AM, Gumienny G, Haas J, Schwede T. *QMEAND* is co – distance constraints applied on model quality estimation. Bioinformatics. 2020;36:1765–71. https://doi.org/10.1093/bioinformatics/btaa058.
Sutherland C, Murakami KS. An introduction to the structure and function of the catalytic core enzyme of Escherichia coli RNA Polymerase. EcoSal Plus. 2018;8:10. https://doi.org/10.1128/ecosalplus.ESP-0004-2018.
Suzuki J, Maliga P. Engineering of the *rpl23* gene cluster to replace the plastid RNA polymerase α subunit with the *Escherichia coli* homologue. Curr Genet. 2000;38:218–25. https://doi.org/10.1007/s002940000141.
Sweet R. Geraniaceae: the natural order of gerania, illustrated by coloured figures and descriptions, comprising the numerous and beautiful mule-varieties cultivated in the gardens of Great Britain, with directions for their treatment. London: Printed for James Ridgway, Piccadilly; 1820-1830. https://doi.org/10.5962/bhl.title.102247.
Tadini L, Jeran N, Peracchio C, Masiero S, Colombo M, Pesaresi P. The plastid transcription machinery and its coordination with the expression of nuclear genome: plastid-encoded polymerase, nuclear- encoded polymerase and the genomes uncoupled 1-mediated retrograde communication. Phil Trans R Soc B. 2020;375:20190399. https://doi.org/10.1098/rstb.2019.0399.
Theeuwen TPJM, Logie LL, Harbinson J, Aarts MGM. Genetics as a key to improving crop photosynthesis. J Exp Bot. 2022;73:3122–37. https://doi.org/10.1093/jxb/erac076.
Tiller N, Bock R. The translational apparatus of plastids and its role in plant development. Mol Plant. 2014;7:1105–20. https://doi.org/10.1093/mp/ssu022.
Tilney-Bassett RAE, Almouslem AB, Amoate HM. Complementary genes control biparental plastid inheritance in *Pelargonium*. Theor Appl Genet. 1992;85:317–24. https://doi.org/10.1007/BF00222876.
Tilney-Bassett RAE, Almouslem AB. Variation in plastid inheritance between *Pelargonium* cultivars and their hybrids. Heredity.1989a; 63:145-53.https://doi.org/10.1038/hdy.1989.86.
Tilney-Bassett RAE, Almouslem AB, Amoatey HM. The complementary gene model for biparental plastid inheritance. In: Boyer CD, Shannon JC, Hardison RC, editors. Physiology, biochemistry, and genetics of nongreen plastids. The American Society of Plant Physiologists 1989b. pp 265-6.
Tilney-Bassett RAE. The genetic evidence for nuclear control of chloroplast biogenesis in higher plants. In: Ellis RJ, editor. Chloroplast biogenesis. (Society for Experimental Biology Seminar Series 21). Cambridge University Press, London, 1984. pp.13-50 .
Van De Kerke SJ, Shrestha B, Ruhlman TA, Weng ML, Jansen RK, Jones CS, et al. Plastome based phylogenetics and younger crown node age in *Pelargonium*. Mol Phylogenet Evol. 2019;137:33–43. https://doi.org/10.1016/j.ympev.2019.03.021.
Van Der Walt JJA, Albers F, Gibby M. Delimitation of *Pelargonium* sect *Glaucophyllum*. Plant Syst Evol. 1990;171:15–26. https://doi.org/10.1007/BF00940594.
Vitales D, Garcia S, Dodsworth S. Reconstructing phylogenetic relationships based on repeat sequence similarities. Mol Phyl Evol. 2020;147:106766. https://doi.org/10.1101/624064.
Wang X, Yaqi A, Pan X, Jianwei X. Functioning of PPR proteins in organelle RNA metabolism and chloroplast biogenesis. Front Plant Sci. 2021;12:627501. https://doi.org/10.3389/fpls.2021.627501.
Waterhouse A, Bertoni M, Bienert S, Studer G, Tauriello G, Gumienny R, et al. SWISS-MODEL: homology modelling of protein structures and complexes. Nucleic Acids Res. 2018;46:W296–303. https://doi.org/10.1093/nar/gky427.
Weihe A, Apitz J, Salinas A, Pohlheim F, Börner T. Biparental inheritance of plastidial and mitochondrial DNA and hybrid variegation in *Pelargonium*. Mol Genet Genomics. 2009;282:587–93. https://doi.org/10.1007/s00438-009-0488-9.
Weng ML, Ruhlman TA, Gibby M, Jansen RK. Phylogeny, rate variation, and genome size evolution of *Pelargonium* (*Geraniaceae*). Mol Phylogenet Evol. 2012;64:654–70. https://doi.org/10.1016/j.ympev.2012.05.026.
Weng ML, Ruhlman TA, Jansen RK. Expansion of inverted repeat does not decrease substitution rates in *Pelargonium* plastid genomes. New Phytol. 2017;214:842–51. https://doi.org/10.1111/nph.14375.
Weng ML, Ruhlman TA, Jansen RK. Plastid-nuclear interaction and accelerated coevolution in plastid ribosomal genes in *Geraniaceae*. Genome Biol Evol. 2016;27(8):1824–38. https://doi.org/10.1093/gbe/evw115.
Westerich LD, Leon Gotsmann VL, Herkt C, Ries F, Kazek T, et al. The versatile interactome of chloroplast ribosomes revealed by affinity purification mass spectrometry. Nucl Acids Res. 2021;49(1). https://doi.org/10.1093/nar/gkaa1192.
Wick RR, Schultz MB, Zobel J, Holt KE. Bandage: interactive visualization of de novo genome assemblies. Bioinformatics. 2015;31:3350–2. https://doi.org/10.1093/bioinformatics/btv383.
Wicke S, Schneeweiss GM, dePamphilis CW, Müller KF, Quandt D. The evolution of the plastid chromosome in land plants: gene content, gene order, gene function. Plant Mol Biol. 2011;76:273–97. https://doi.org/10.1007/s11103-011-9762-4.
Williams-Carrier R, Zoschke R, Belcher S, Pfalz J, Barkan A. A major role for the plastid-encoded RNA polymerase complex in the expression of plastid transfer RNAs. Plant Physiol. 2014;164:239–48. https://doi.org/10.1104/pp.113.228726.
Yao JL, Cohen D. Multiple gene control of plastome-genome incompatibility and plastid DNA inheritance in interspecific hybrids of *Zantedeschia*. Theor Appl Genet. 2000;101:400–6. https://doi.org/10.1007/s001220051496.
Yao JL, Cohen D, Rowland RE. Plastid DNA inheritance and plastome-genome incompatibility in interspecific hybrids of *Zantedeschia* (Araceae). Theor Appl Genet. 1994;88:255–60. https://doi.org/10.1007/BF00225906.
Zhang Y, Feng Y, Chatterjee S, Tuske S, Ho MX, Arnold E, et al. Structural basis of transcription initiation. Science. 2012;338:1076–88. https://doi.org/10.1126/science.1227786.
Zhang J, Ruhlman TA, Mower JP, Jansen RK. Comparative analyses of two *Geraniaceae* transcriptomes using next-generation sequencing. BMC Plant Biol. 2013;13:228. https://doi.org/10.1186/1471-2229-13-228.
Zhang J, Ruhlman T, Sabir J, Blazier J, Jansen R. Coordinated rates of evolution between interacting plastid and nuclear genes in *Geraniaceae*. Plant Cell. 2015;27:563–73. https://doi.org/10.1105/tpc.114.134353.
Zhang JJ, Ruhlman TA, Sabir JSM, Blazier JC, Weng M-L, Park S, et al. Coevolution between nuclear-encoded DNA replication, recombination, and repair genes and plastid genome complexity. Genome Biol Evol. 2016;3:622–34. https://doi.org/10.1093/gbe/evw033.
Zoschke R, Bock R. Chloroplast translation: structural and functional organization, operational control, and regulation. Plant Cell. 2018;30:745–70. https://doi.org/10.1105/tpc.18.00016.

Publisher's Note